Progress In Electromagnetics Research, Vol. 139, 229–245, 2013

DESIGN OF A NOVEL SUPER WIDE BAND CIRCULAR-HEXAGONAL FRACTAL ANTENNA

Mohammad A. Dorostkar[1, 2], Mohammad T. Islam[2, *], and Rezaul Azim[2],

[1]Department of Electrical, Electronic and Systems Engineering, Universiti Kebangsaan Malaysia, UKM Bangi 43600, Malaysia

[2]Institute of Space Science (ANGKASA), Universiti Kebangsaan Malaysia, UKM Bangi 43600, Malaysia

Abstract—In this paper, a novel circular-hexagonal Fractal antenna is investigated for super wide band applications. The proposed antenna is made of iterations of a hexagonal slot inside a circular metallic patch with a transmission line. A partial ground plane and asymmetrical patch toward the substrate are used for designing the antenna to achieve a super wide bandwidth ranging from 2.18 GHz to 44.5 GHz with a bandwidth ratio of 20.4 : 1. The impedance bandwidth and gain of the proposed antenna are much better than the recently reported super wideband antennas which make it appropriate for many wireless communications systems such as ISM, Wi-Fi, GPS, Bluetooth, WLAN and UWB. Details of the proposed antenna design are presented and discussed.

1. INTRODUCTION

Nowadays, antenna with good characteristics, low cost and small size is an important component and plays a key role in wireless communication [1–10]. Besides exploiting the frequency band of 3.1–10.6 GHz for ultrawideband applications, the present users of wireless communication technology are eagerly searching for a super wide band antenna (SWB) to cover both the short and long range transmission for ubiquitous applications [11]. SWB technology is becoming more and more important to many potential applications due to larger channel capacity, higher time precision etc. An antenna with the bandwidth

Received 5 March 2013, Accepted 15 April 2013, Scheduled 24 April 2013

* Corresponding author: Mohammad Tariqul Islam (titareq@yahoo.com).

ratio larger than 10 : 1 for impedance bandwidth at 10 dB return loss is called super wideband [12].

Different techniques and methods have already been proposed to achieve super wide operating band. In recent years, there has been an increasing amount of literature on SWB antenna [13–21]. For example a compact semi-elliptical patch antenna fed by a tapered coplanar waveguide was designed in [13]. With a measured bandwidth ratio of 19.7 : 1, the proposed antenna is suitable to operate within frequencies of 0.46 GHz to 9.07 GHz. In [14], a half circular antipodal slot antenna with a range of super wideband frequencies between 0.8 GHz to 7 GHz was presented. A planar asymmetrical dipole antenna of circular shape was proposed in [15]. With a dimension of 90 mm × 135 mm, the proposed antenna achieved an operating bandwidth ranging from 0.79 to 17.46 GHz. An asymmetrical super-wideband dipole antenna is implemented in [16]. A novel SWB antenna that achieved a frequency band between 5 GHz to 150 GHz is proposed in [17]. Despite of huge bandwidth it is not suitable for lower frequency bands such as WiMAX and S band communication. In [18], a compact super wideband monopole antenna with switchable dual band-notched characteristics was proposed for 3 to 33 GHz band. However, the performance of this antenna was not validating experimentally. A disc shape planar super wide band antenna with C-like slots was presented in [19]. With an overall dimension of 30 mm × 29.1 mm, the designed antenna achieved to operate within 3–32 GHz. An extremely wideband monopole antenna with triple-band notched characteristics was presented in [20]. With a size of 150 mm × 150 mm, the designed antenna achieved a bandwidth ranging from 0.72–25 GHz with three notch band for WLAN and X-band. In [21], a monopole antenna with super-wideband was proposed. However, it's three dimensional structure makes it difficult to be integrated into portable devices. Besides, the antennas proposed in [19–21] do not cover K-band which opens a new arena to design antenna that covers S, C, X, Ku, K and Ka bands.

Other than the monopole antennas, one of the effective methods to achieve SWB is the fractal geometry. Self similarity and space filling are two common important properties of fractal geometry. Self similarity leads to wide band while space filling increases the electrical length [22–39]. In [26], a super wide band fractal antenna had been modeled and simulated for super wideband application. By using a normal square loop the proposed antenna achieved a super wide frequency band ranging from 20 GHz to 60 GHz. However its performance has not been validated experimentally and it is not suitable for microstrip technology. Based on an iterative octagon, a

new super wideband fractal antenna was proposed in [27]. With an overall dimension of 60 mm × 60 mm, the proposed antenna achieved a huge bandwidth of 40 GHz ranging from 10–50 GHz and is not suitable for L, S, C and UWB band applications. A new fractal antenna for super wideband applications was presented in [28]. By applying the fractal generator to square loop elements, the proposed antenna achieved a bandwidth of 29 GHz (1–30 GHz). However its application in portable wireless devices is limited due to its wire shape and large dimensions. In [11], a compact monopole antenna was proposed for SWB applications. By embedding a semielliptical fractal-complementary slot into the asymmetrical ground plane, the designed antenna was able to operate from 1.44 to 18.8 GHz. However, the antenna has a large dimension with an area of 2695 mm^2 (77 mm × 35 mm).

In this paper, a novel super wide band fractal antenna based on circular-hexagonal geometry with an electrical dimension $0.33\lambda \times 0.23\lambda \times 0.18\lambda$ (where λ is the lower edge frequency of the operating band) is proposed. The iterations of a hexagonal slot inside a circular metallic patch with a transmission line helps to achieve super wide impedance bandwidth. The symmetric radiation patterns and stable gain make the proposed suitable for being used in various wireless applications such as ISM (2400–2483 MHz), Wi-Fi (2400 MHz), GPS (2400 MHz), Bluetooth (2400–2500 MHz), WLAN (2.4–2.48 GHz, 5.15–5.85 GHz) and UWB (3100–10600 MHz). Compared to the antennas reported earlier, the proposed antenna is compact, simple and easy to fabricate.

2. ANTENNA DESIGN

The proposed antenna structure composed of a circular metallic patch, in which circular arrow fractal slots are cut through the length of a central hexagonal slot. The configuration is made of iterations of a circular slot inside a hexagonal metallic patch, up to the sixth iterations. The partial ground plane is split into two square metallic plates. Furthermore, the proposed radial arrow fractal slots cause the path lengths of surface currents on the patch which leads to the multi and wide band antenna. Figure 1 shows the design procedure of the proposed Fractal structure geometry.

Four parameters are considered for design including d (different length between hexagonal and circulars), L_t (length of transmission line), L_G (length of ground plane), W (width of the transmission line). According to the relations 1 and 2, R_i is depended on d_i and also the differing length between L_t and L_G is related to h (gap between

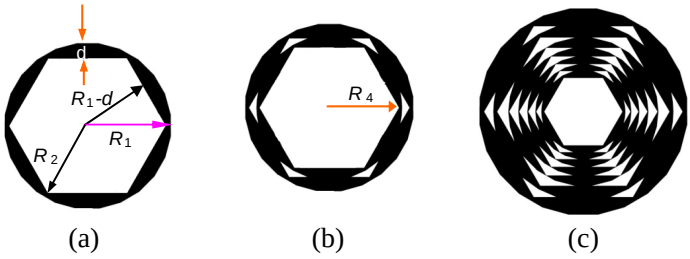

Figure 1. Design procedure of proposed fractal structure geometry. (a) Base shape. (b) First iteration $R_4 = \frac{2}{\sqrt{3}}(R_1 - 2d)$. (c) Final shape.

transmission line and ground plan). The parameters mentioned above are considered with a parameter vector called $\lambda = \{L_t, L_G, W, d_i; i = 1, 2, 3, \ldots, 7\}$.

$$R_{i+1} = \frac{2}{\sqrt{3}}\left[R_1 - (i \times d_1)\right], \quad i = 1, 2, \ldots \tag{1}$$

$$h = L_t - L_G \tag{2}$$

The proposed antenna is fabricated on Rogers/Duroid 5870 substrate of 31 mm × 45 mm with thickness 1.575 mm, $\varepsilon_r = 2.3$ and a loss tangent $\delta = 0.0012$.

The configuration of the proposed antenna is shown in Figure 2. Figure 2(a) depicts the radiating patch where R_1 is the length of first hexagonal; L_t is the length of transmission line and W is the width of the transmission line. The ground plane is shown in Figure 2(b) where L_G is the side length of the ground plane. A rectangular slot has been inserted at the top edge of the ground plane.

Since the iterations play a vital role in achieving super wide

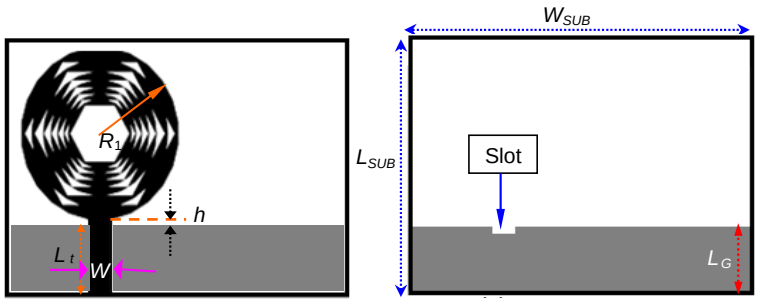

Figure 2. Geometry of the proposed patch antenna.

bandwidth, the effect of different iterations on impedance bandwidth is shown in Figure 3. It is seen that the antenna with higher iterations exhibits better bandwidth, so we continue the iterations to the six steps to achieve a high performance.

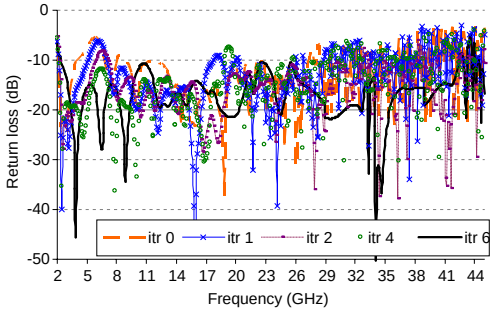

Figure 3. Variation of return loss for various iterations.

3. ANTENNA SPECIFICATIONS

The geometric construction of circular-hexagonal Fractal shape starts with a circular shape that is subtracted with hexagonal shape is shown in Figure 2.

Relation 1 shows the iterative function system (IFS) to define the generator:

$$W\begin{pmatrix} x_{new} \\ y_{new} \end{pmatrix} = \begin{pmatrix} \cos\theta & 0 \\ 0 & \sin\theta \end{pmatrix} \begin{pmatrix} x_{old} \\ y_{old} \end{pmatrix} - \begin{pmatrix} n \times d \times \cos\theta \\ n \times d \times \sin\theta \end{pmatrix} \tag{3}$$

$$W(A) = \bigcup_{1}^{N} W_n(A) \tag{4}$$

where θ is the angle toward the center and n is called the number of iterations.

The dimension of the perimeter of a circle is equal 1 ($D = 1$) and circle area is called S_{circle} with dimension of two ($D = 2$), so the dimensions of the proposed shape are between 1 and 2 ($1 < D < 2$). Due to existing of two types of shapes (circular and hexagonal) as shown in Figure 4, the dimension of the proposed geometry is not able to be figured out only by one scale factor. In the first step, the equivalent circular shape with hexagonal shape should be calculated according to the relation (6). Then the dimension of the new proposed fractal shape can be computed according to the relation (8). R_1/R_n is

scale factor where R_1 is the radius of the first circle and R_n is the radius of the equivalent circle with the hexagonal length of nth iterations. S_n is the area of nth iterations that is determined with relation (7). The circle area S_{circle} is define as

$$S_{circle} = \pi R_n^2 \tag{5}$$

R_n, the radius of the corresponding circle with a hexagonal length of nth iterations can be written as

$$R_n = \sqrt{\frac{2\sqrt{3}}{\pi}} \left[R_1 - (n \times d)\right] \tag{6}$$

The circular area corresponding to area of circular-hexagonal Fractal of nth iterations is

$$S_n = \pi R^2 \tag{7}$$

$$D = \frac{\log\left(\frac{S_{circle} - S_n}{S_n}\right)}{\log\left(\frac{R_1}{R_n}\right)} \tag{8}$$

The first design is done with $R_1 = 10.39\,\text{mm}$ and $d = 0.3\,\text{mm}$ that d is constant for all iterations. The dimensions for proposed geometry to 6 iterations are arranged in Table 1. It can be observed that increasing iterations increase the dimension, so lead to increasing the electrical length.

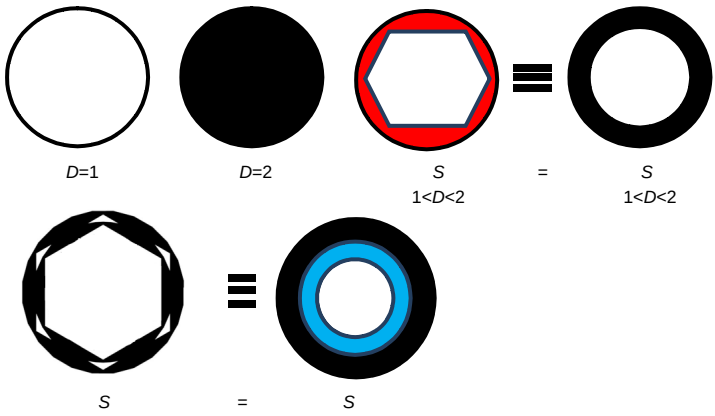

Figure 4. Proposed equivalent shape for dimension calculation.

Table 1. Dimension of the proposed fractal geometry for all iterations.

Iteration	Base shape	First	Second	Third	Fourth
Dimension	1.5524	1.6006	1.6439	1.6829	1.7179
Iteration	Fifth	Sixth			
Dimension	1.7495	1.7779			

4. PARAMETRIC ANALYSIS

A parametric analysis is conducted in order to optimize the antenna parameters. It helps to survey the effects of the different parameters on impedance bandwidth. Some algorithm such as genetic algorithm (GA) and particle swarm optimization (PSO) can use in order to find an antenna configuration that fit a set of user-defined constraint on the size and the impedance-matching behavior. For optimization in this study genetic algorithm is applied. To do so, firstly the parameter of $\lambda_1 = \{L_t, L_G, W\}$ is optimized then $\lambda_2 = \{d_i: i = 1, 2, \ldots, 7\}$. The strategy of the synthesis procedure is the minimizing of the following function:

$$G_\lambda(f) = S_\lambda(f) + 10 < 0 \tag{9}$$

where; $S_\lambda(f)$ is the function of return loss with specified parameters of the proposed antenna and $G_\lambda(f)$ is the optimized function that has larger bandwidth.

The variations of the return loss with λ_1 (i.e., L_t, L_G and W) are depicted in Figure 5. In this stage, λ_2 is constant in which $R_1 = 10.45\,\text{mm}$ and $d_i = 0.3\,\text{mm}$ ($i = 1, 2, \ldots, 6$). It can be observed that decreasing and increasing of each parameter of λ_1 lead to decrease the bandwidth of the specified value, and also increasing or decreasing λ_1 do not affect the lower resonance frequencies. λ_1 is important for enhancing the bandwidth in high frequency. Based on the observations using genetic algorithm, $\lambda_1 = \{L_t = 9.2137\,\text{mm}, L_G = 8.7\,\text{mm}, W = 2.2923\,\text{mm}\}$ is the best vectors for achieving widest bandwidth.

In the second step of the optimization process with λ_2 (i.e., d_i: $i = 1, 2, \ldots, 7$), the value of λ_1 is taken as $\lambda_1 = \{L_t = 9.2137\,\text{mm}, L_G = 8.7\,\text{mm}$ and $W = 2.923\,\text{mm}\}$ which is the optimized value in the first step. The variations of the return loss for different values of λ_2 are shown in Figure 6. It is observed that decreasing and increasing of λ_2 parameters have more effect at high frequencies. Also increasing the λ_2 parameters lead to decrease the low edge of frequency about 0.2 GHz. Table 2 summaries the variations of λ_2 parameters from which it is clear that λ_2 with a good impedance bandwidth can be taken as the optimized values to give wider bandwidth.

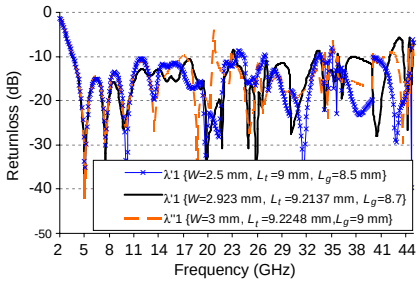

Figure 5. Effect of λ_1 on return loss.

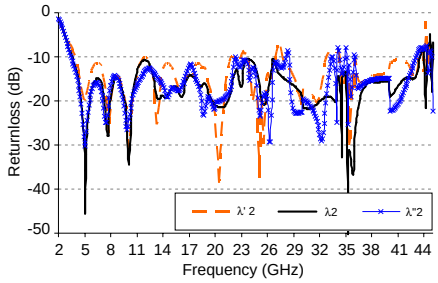

Figure 6. Effect of λ_2 on return loss.

Table 2. Variations of values for all λ_2 parameters.

λ_2'	λ_2	λ_2''
$R_1 = 10.45\,\text{mm}$	$R_1 = 10.39\,\text{mm}$	$R_1 = 10.45\,\text{mm}$
$d_1 = 0.3\,\text{mm}$	$d_1 = 0.5\,\text{mm}$	$d_1 = 0.5\,\text{mm}$
$d_2 = 0.3\,\text{mm}$	$d_2 = 0.4\,\text{mm}$	$d_2 = 0.4\,\text{mm}$
$d_3 = 0.3\,\text{mm}$	$d_3 = 0.1\,\text{mm}$	$d_3 = 0.4\,\text{mm}$
$d_4 = 0.3\,\text{mm}$	$d_4 = 0.1\,\text{mm}$	$d_4 = 0.45\,\text{mm}$
$d5 = 0.3\,\text{mm}$	$d_5 = 0.1\,\text{mm}$	$d_5 = 0.5\,\text{mm}$
$d_6 = 0.3\,\text{mm}$	$d_6 = 0.1\,\text{mm}$	$d_5 = 0.45\,\text{mm}$
$d_7 = 0.3\,\text{mm}$	$d_7 = 0.3\,\text{mm}$	$d_7 = 0.5\,\text{mm}$

The gap between transmission line and the ground plane, h plays a vital role in achieving super wideband width. The variations of return loss for different values of h with $L_t = 9.2137\,\text{mm}$ and $W = 2.923\,\text{mm}$ is depicted in Figure 7. It can be observed from the plot that increasing of the h lead to decrease the return loss in low frequency and close to the low resonance frequencies. It is also seen that increasing and decreasing of h from certain value leads to create a stop band at high frequencies. A gap of $0.5137\,\text{mm}$ can maintain the good impedance bandwidth with better return loss values.

The impedance bandwidth characteristics of the proposed antenna can be enhanced by embedding a rectangular slot at the top of edge ground. It is observed that the operating bandwidth is greatly dependent on the insertion of a slot at the top edge of the ground plane. This phenomenon occurs because the slot acts as a current perturbation on the ground plane resulting in an increment of bandwidth due to extra electromagnetic coupling between the patch

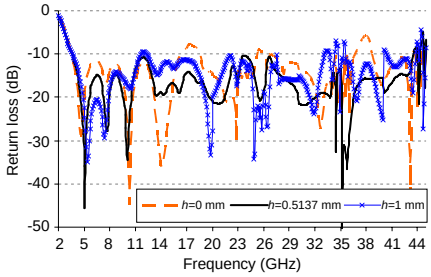

Figure 7. Effect of h on return loss.

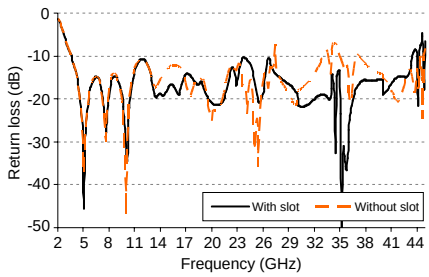

Figure 8. Effect of slot on return loss characteristics.

and the ground plane. It also reduces the size of the ground plane. It is observed from Figure 8 that, the inclusion of a rectangular slot of 3 mm × 0.817 mm in the ground plane increases the bandwidth especially at the higher frequency band.

The variation of the return loss with substrate length, L_{SUB} with fixed patch width is shown in Figure 9. It can be observed from the plot that increasing of L_{SUB} with fixed patch lead to decrease the edge lower of frequencies. Also it is seen that shifting the patch from the substrate center lead to decrease the lower edge of frequencies of the operating band. Increasing the L_{SUB} value and asymmetrical position of the patch toward the substrate center lead to decrease the lower edge frequencies and moves the first resonance frequency from 4.8 GHz to 2.5 GHz. Therefore, an L_{SUB} equal to 45 mm is chosen to be the optimized value to achieve widest bandwidth.

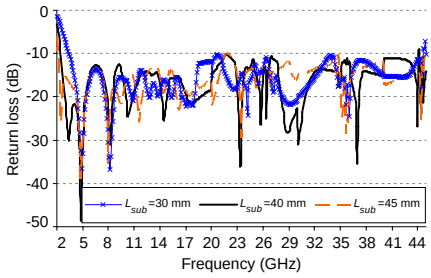

Figure 9. Effect of L_{SUB} on return loss.

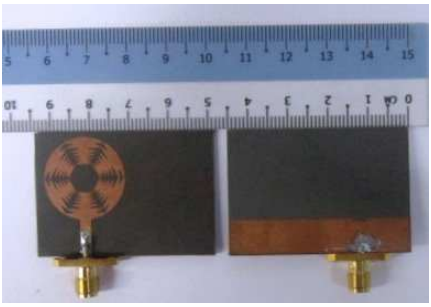

Figure 10. Photograph of the realized Fractal antenna.

5. RESULTS AND DISCUSSION

The characteristics of the proposed antenna have been analyzed by high frequency simulation software based on finite element method. A prototype with optimized dimensions tabulated in Table 3 has subsequently been fabricated for experimental verification and shown in Figure 10. The antenna performances have been measured in an anechoic chamber using far field antenna measurement system and Agilent E8362C Vector Network Analyzer. The experimental setup was calibrated carefully by considering the effect of feeding cable using an Agilent digital calibration kit (85052D — 3.5 mm Economy Calibration Kit) that can measure till 20 GHz.

Table 3. Optimized parameters of the proposed antenna.

Parameter	Value (mm)	Parameter	Value (mm)	Parameter	Value (mm)
L_t	9.2137	d_1	0.5	d_5	0.1
L_G	8.7	d_2	0.4	d_6	0.1
W	2.923	d_3	0.1	d_7	0.3
R_1	10.391	d_4	0.1		

The simulated and measured return losses and VSWR of the proposed antenna are depicted in Figure 11 and Figure 12 respectively. Figure 11 and Figure 12 show that the measured impedance bandwidth (return loss ≤ -10 dB, VSWR ≤ 2) of the proposed antenna is ranging from 2.18 to 20 GHz (Maximum limit of network analyzer). The disparity between the measured and simulated results especially at edge frequencies is attributed to manufacturing tolerance and imperfect soldering effect of the SMA connector.

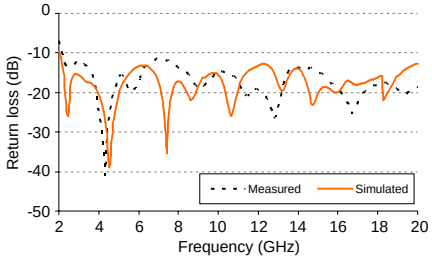

Figure 11. Measured and simulated return loss of the proposed antenna.

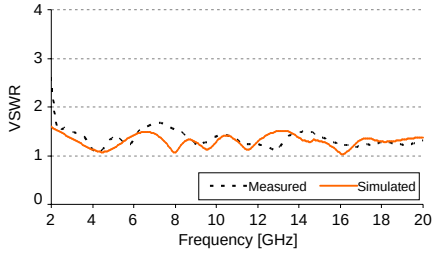

Figure 12. Measured and simulated VSWR of the proposed antenna.

Figure 13 shows the peak gain of the proposed antenna in the frequency range of 2–20 GHz. It can be observed from the plot that the antenna has a good average gain of 4.38 dBi. The maximum peak gain is about 7 dBi at around 20 GHz.

The radiation efficiency plot of the proposed antenna is depicted in Figure 14. The result shows that the maximum radiation efficiency of the proposed antenna is 99.99% at 16.8 GHz and the average efficiency is 98.8% across the entire operating band.

We also compare the efficiency between theoretical and practical. Figure 15 shows the efficiency based on wheeler and Chu formula [40] that is shown in relation 10 and 11. A theoretical efficiency of 99.99 % has been achieved by the proposed antenna

$$Q = \left(\frac{1}{ka} + \frac{1}{(ka)^3}\right) \tag{10}$$

k is wave number and $a = 4.5$ cm is the sphere encloses of the proposed antenna

$$\eta = \frac{R_{rad}}{R_{rad} + R_{loss}} \approx \frac{1}{1 + Q \cdot \tan\delta} \tag{11}$$

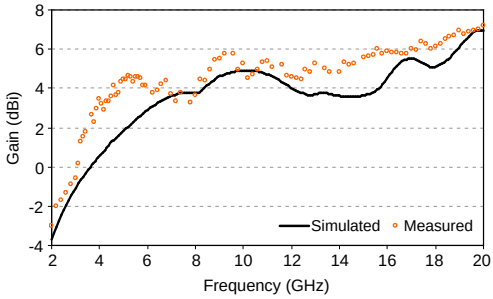

Figure 13. Peak gain of the proposed antenna.

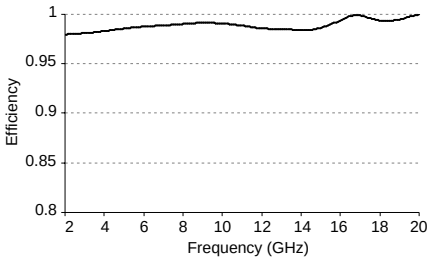

Figure 14. Efficiency of the proposed antenna.

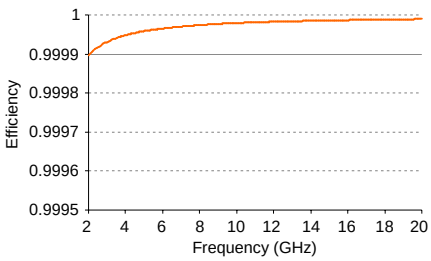

Figure 15. Theoretical efficiency of the proposed antenna.

It is seen that on average the practical plot falls down by 1.1% in comparison to the theatrical one.

The radiation patterns of the proposed antenna are measured at three resonance frequencies of 2.5 GHz, 4.8 GHz and 9.3 GHz, and are depicted in Figure 16. It is observed from the plot that at lower

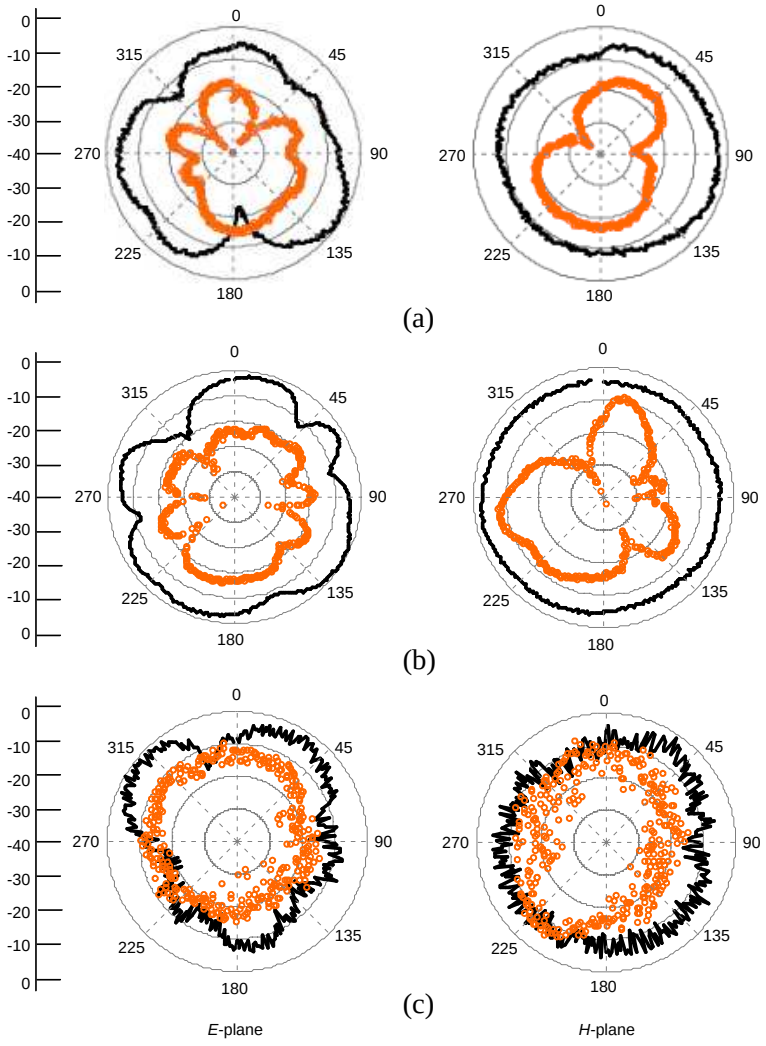

Figure 16. Measured radiation patterns at (a) 2.5 GHz, (b) 4.8 GHz, and (c) 9.3 GHz (Solid line: co-polarized field, Circled line: cross-polarized field).

frequency of 2.5 GHz and 4.8 GHz, the co-polarized radiation patterns are omnidirectional in H-planes. In E-plane, at lower frequencies some null is introduced in the patterns. As the frequency increases, the higher order current modes are excited and patterns become slightly directional. Although the cross polarization level increases and some nulls are observed at higher frequencies due to the diversified electric current distribution, the proposed antenna exhibits stable radiation patterns throughout the operating band and the patterns are similar to that of typical monopole antennas [41, 42]. At higher frequencies the patterns resulted from the measurements have some ripples in amplitude due to many reflections into the field between the AUT and reference antenna. The reflections may come from the room floor and ceiling, chamber scattering and track inside the anechoic chamber.

6. CONCLUSION

A novel hexagonal-circular Fractal antenna has been proposed and prototyped for super wideband wireless applications. A design evolution and a parametric analysis with genetic algorithm of the proposed antenna are presented to provide information for designing, optimizing and to understand the fundamental radiation mechanism of the proposed antenna. The iterations of a hexagonal slot inside a circular metallic patch helps to achieve wide impedance bandwidth. It is observed from antenna performance that the proposed antenna achieved a super wideband ranging from 2.18 to 44.5 GHz. The symmetric omnidirectional radiation patterns with a stable gain make the proposed antenna suitable for many applications such as GPS, IMT-2000/UMTS, ISM, Wi-Fi, Bluetooth and UWB. The design of the proposed antenna is simple, ease to fabricate, and very suitable to integrate into microwave circuitry for planar structure.

REFERENCES

1. Kang, W., K. H. Ko, and K. Kim, "A compact beam reconfigurable antenna for symmetric beam switching," *Progress In Electromagnetics Research*, Vol. 129, 1–16, 2012.
2. Sze, J.-Y. and S.-P. Pan, "Design of broadband circularly polarized square slot antenna with a compact size," *Progress In Electromagnetics Research*, Vol. 120, 513–533, 2011.
3. Peng, H.-L., W.-Y. Yin, J.-F. Mao, D. Huo, X. Hang, and L. Zhou, "A compact dual-polarized broadband antenna with hybrid beam-forming capabilities," *Progress In Electromagnetics Research*, Vol. 118, 253–271, 2011.

4. Weng, W.-C. and C.-L. Hung, "Design and optimization of a logo-type antenna for multiband applications," *Progress In Electromagnetics Research*, Vol. 123, 159–174, 2012.
5. Ban, Y.-L., J.-H. Chen, S.-C. Sun, J. L.-W. Li, and J.-H. Guo, "Printed wideband antenna with chip-capacitor-loaded inductive strip for LTE/GSM/UMTS WWAN wireless USB dongle applications," *Progress In Electromagnetics Research*, Vol. 128, 313–329, 2012.
6. Tiang, J.-J., M. T. Islam, N. Misran, and J. S. Mandeep, "Circular microstrip slot antenna for dual-frequency RFID application," *Progress In Electromagnetics Research*, Vol. 120, 499–512, 2011.
7. Xie, J.-J. Y.-Z. Yin, J. Ren, and T. Wang, "A wideband dual-polarized patch antenna with electric probe and magnetic loop feeds," *Progress In Electromagnetics Research*, Vol. 132, 499–515, 2012.
8. Azim, R., M. T. Islam, J. S. Mandeep, and A. T. Mobashsher, "A planar circular ring ultra-wideband antenna with dual band-notched characteristics," *Journal of Electromagnetic Waves and Applications*, Vol. 26, Nos. 14–15, 2022–2032, 2012.
9. Amin, Y., Q. Chen, L.-R. Zheng, and H. Tenhunen, "Design and fabrication of wideband archimedean spiral antenna based ultra-low cost "green" modules for RFID sensing and wireless applications," *Progress In Electromagnetics Research*, Vol. 130, 241–256, 2012.
10. Chen, A.-X., T.-H. Jiang, Z. Chen, and D. Su, "A novel low-profile wideband UHF antenna," *Progress In Electromagnetics Research*, Vol. 121, 75–88, 2011.
11. Chen, K. R., C. Y. D. Sim, and J. S. Row, "A compact monopole antenna for super wideband applications," *IEEE Antennas and Wireless Propagation Letters*, Vol. 10, 488–491, 2011.
12. Tran, D., P. Aubry, A. Szilagyi, I. E. Lager, O. Yarovyi, and L. P. Ligthart, "On the design of a super wideband antenna," 399–426, *Ultra Wideband,* Boris Lembrikov (ed.), InTech Publication, 2011, ISBN: 978-953-307-139-8.
13. Yan, X. R., S. S. Zhong, and X. X. Yang, "Compact printed monopole antenna with super-wideband," *Proceedings of the International Symposium on Microwave, Antenna, Propagation and EMC Technologies for Wireless Communications*, 605–607, China, 2007.
14. Lu, W. and H. Zhu, "Super-wideband antipodal slot antenna," *Proceedings of the Asia Pacific Microwave Conference*, 1894–1897, Singapore, 2009.

15. Barbarino, S. and F. Consoli, "Study on super-wideband planar asymmetrical dipole antennas of circular shape," *IEEE Transactions on Antennas and Propagation*, Vol. 58, No. 12, 4074–4078, 2010.
16. Jin, X. H., X. D. Huang, C. H. Cheng, and L. Zhu, "Super-wideband printed asymmetrical dipole antenna," *Progress In Electromagnetics Research Letters*, Vol. 27, 117–123, 2011.
17. Tran, D., A. Szilagyi, I. E. Lager, P. Aubry, L. P. Ligthart, and A. Yarovoy, "A super wideband antenna," *Proceedings of the 5th European Conference on Antennas and Propagation*, 2656–2660, Italy, 2011.
18. Almalkawi, M., M. Westrick, and V. Devabhaktuni, "Compact super wideband monopole antenna with switchable dual band-notched characteristics," *Proceedings of the Asia-Pacific Microwave Conference*, 723–725, Taiwan, 2012.
19. Mahmud, M. S. and S. Dey, "Design and performance analysis of a compact and conformal super wide band textile antenna for wearable body area applications," *Proceedings of the 6th European Conference on Antennas and Propagation*, 1–5, Czech Republic, 2012.
20. Liu, J. K., P. Esselle, S. G. Hay, and S. S. Zhong, "Study of an extremely wideband monopole antenna with triple band-notched characteristics," *Progress In Electromagnetics Research*, Vol. 123, 143–158, 2012.
21. Lau, K. L., K. C. Kong, and K. M. Luk, "Super-wideband monopolar patch antenna," *Electronics Letters*, Vol. 44, No. 12, 716–718, 2008.
22. Werner, D. H. and S. Ganguly, "An overview of fractal antenna engineering research," *IEEE Antennas and Propagation Magazine*, Vol. 45, No. 1, 38–57, 2003.
23. Cohen, N., "Fractal antenna application in wireless telecommunications," *Proceedings of the Electronics Industries Forum of New England*, 43–49, 1997.
24. Gouyet, J. F., *Physics and Fractal Structures*, Springer, Paris, 1996.
25. Werner, D. H., R. L. Haupt, and P. L. Werner, "Fractal antenna engineering: The theory and design of fractal antenna arrays," *IEEE Antennas and Propagation Magazine,* Vol. 41, No. 5, 37–58, 1999.
26. Azari, A., "Super wideband fractal antenna design," *Proceedings of the International Symposium on Microwave, Antenna, Propa-*

gation and EMC Technologies for Wireless Communications, 242–245, China, 2009.

27. Azari, A., "A new super wideband fractal microstrip antenna," *IEEE Transactions on Antennas and Propagation*, Vol. 59, No. 5, 1724–1727, 2011.
28. Azari, A., "A new fractal antenna for super wideband applications," *PIERS Proceedings*, 885–888, Cambridge, USA, Mar. 5–8, 2010.
29. Ghatak, R., A. Karmakar, and D. R. Poddar, "A circular shaped Sierpinski carpet fractal UWB monopole antenna with band rejection capability," *Progress In Electromagnetics Research C*, Vol. 24, 221–234, 2011.
30. Li, D. and J.-F. Mao, "Koch-like sided Sierpinski gasket multifractal dipole antenna," *Progress In Electromagnetics Research*, Vol. 126, 399–427, 2012.
31. Li, D. and J.-F. Mao, "Sierpinskized Koch-like sided multifractal dipole antenna," *Progress In Electromagnetics Research*, Vol. 130, 207–224, 2012.
32. Levy, M., S. Bose, A. V. Dinh, and D. Sriram Kumar, "A novelistic fractal antenna for ultra wideband (UWB) applications," *Progress In Electromagnetics Research B*, Vol. 45, 369–393, 2012.
33. Li, Y.-S., X.-D. Yang, C.-Y. Liu, and T. Jiang, "Analysis and investigation of a cantor set fractal UWB antenna with a notch-band characteristic," *Progress In Electromagnetics Research B*, Vol. 33, 99–114, 2011.
34. Aziz, R. S., M. A. S. Alkanhal, and A.-F. Sheta, "Multiband fractal-like antennas," *Progress In Electromagnetics Research B*, Vol. 29, 339–354, 2011.
35. Li, Y.-S., X.-D. Yang, C.-Y. Liu, and T. Jiang, "Analysis and investigation of a cantor set fractal UWB antenna with a notch-band characteristic," *Progress In Electromagnetics Research B*, Vol. 33, 99-114, 2011.
36. Lin, S., L.-Z. Wang, Y. Wang, X.-Y. Zhang, and H.-J. Zhang, 'Design and analysis of a circular polarization microstrip antenna with koch fractal edges," *Progress In Electromagnetics Research Letters*, Vol. 34, 9–19, 2012.
37. Kimouche, H. and H. Zemmour, "A compact fractal dipole antenna for 915 MHz and 2.4 GHz RFID tag applications," *Progress In Electromagnetics Research Letters*, Vol. 26, 105–114, 2011.
38. Malik, J. and M. V. Kartikeyan, "A stacked equilateral

triangular patch antenna with Sierpinski gasket fractal for WLAN applications," *Progress In Electromagnetics Research Letters*, Vol. 22, 71–81, 2011.

39. Ghatak, R., A. Karmakar, and D. R. Poddar, "Hexagonal boundary Sierpinski carpet fractal shaped compact ultrawideband antenna with band rejection functionality," *International Journal of Electronics and Communications*, Vol. 67, No. 3, 250–255, 2013.
40. Sievenpiper, D. F., D. C. Dawson, M. M. Jacob, T. Kanar, K. Sanghoon, J. Long, and R. G. Quarfoth, "Experimental validation of performance limits and design guidelines for small antennas," *IEEE Transactions on Antennas and Propagation*, Vol. 60, No. 1, 8–19, 2012.
41. Azim, R. and M. T. Islam, "Compact planar UWB antenna with band notch characteristics for WLAN and DSRC," *Progress In Electromagnetics Research*, Vol. 133, 391–406, 2013.
42. Islam, M. T., R. Azim, and A. T. Mobashsher, "Triple band-notched planar UWB antenna using parasitic strips," *Progress In Electromagnetics Research*, Vol. 129, 161–179, 2012.